

Sweep frequency response analysis for diagnosis of low level short circuit faults on the windings of power transformers: An experimental study

Vahid Behjat^{a,b,*}, Abolfazl Vahedi^a, Alireza Setayeshmehr^c, Hossein Borsi^c, Ernst Gockenbach^c

^a Center of Excellence for Power System Automation and Operation, Iran University of Science & Technology, Tehran, Iran

^b Department of Electrical Engineering, Engineering Faculty, Azarbaijan University of Tarbiat Moallem, Tabriz, Iran

^c Institute of Electric Power Systems, High Voltage Engineering Section (Schering-Institute), Leibniz Universität Hannover, Germany

ARTICLE INFO

Article history:

Received 7 April 2011

Received in revised form 29 February 2012

Accepted 10 March 2012

Available online 7 May 2012

Keywords:

Power transformer

Low-level short circuit fault

Diagnosis

SFRA

Transfer function method

ABSTRACT

This contribution is aimed at obtaining diagnosis criteria for detection of low-level short circuit faults throughout sweep frequency response analysis (SFRA) measurements on the transformer windings. Significant advantages would accrue by early detection of low level short circuit faults within the transformer, since if not quickly detected, they usually develop into more serious faults which result in irreversible damage to the transformer and the electrical network, unexpected outages and the consequential costs. A Finite Element Model (FEM) of the tested transformer has been developed to assist in justifying the modifications of the winding frequency response as a result of fault occurrence. Successful operation of the SFRA method in precisely detecting interturn faults along the transformer windings, even down to a few shorted turns on the winding, is proved through a large number of experiments and measurements. Improving the interpretation of the SFRA measurements needs complementary statistical indicators. The usage of correlation coefficient and spectrum deviation for comparison of the frequency responses obtained through SFRA measurements provides quantitative indicators of the fault presence on the transformer windings and also the fault severity level in the shorted turns.

© 2012 Elsevier Ltd. All rights reserved.

1. Introduction

Power transformers are the most expensive and strategically important elements of any electrical power generation and transmission system. However, they do suffer from internal winding faults principally due to insulation failure; these faults must be quickly and accurately detected and the appropriate action taken to isolate the faulty transformer from the rest of the power system [1]. If not quickly detected, these faults can propagate and lead to catastrophic phase to ground or phase to phase faults resulting in a complete transformer breakdown which in turn generate substantial costs for repair or replacement and financial loss due to the power outage [2]. Most power utilities are therefore highly motivated to detect interturn short circuit fault in its earliest stage to prevent further damage to the transformer and electrical network. Conventional methods for early detection of failures in power transformers such as dissolved gas in oil analysis, partial discharge analysis and power factor tests, display considerable limitations in detection of interturn faults on the transformer windings [3]. Also the problem with the lastly developed power transformers

assessment methods is that they just only give a general indication of the internal status of the transformer and do not permit the detection of interturn winding faults [4].

Frequency response analysis as one of the well-recognized methods for on-site diagnosis of power transformers is based on the fact that every transformer winding has a unique signature of its transfer function which is sensitive to change in the parameters of the winding, namely resistance, inductance and capacitance. Any geometrical or electrical changes within the transformer due to internal faults which have an effect on the capacitive or inductive behavior of a transformer winding cause a change in the transfer function of the winding and consequently a modification of its frequency response. Since the pioneering work of Dick and Erven at Ontario Hydro Research Laboratories in Canada in the late 1970s, FRA has been widely applied to power transformers to investigate mechanical integrity of the windings [6]. There are two ways for making frequency response analysis (FRA) measurements: sweep frequency response analysis (SFRA) and low voltage impulse method (LVI). Many early practitioners tried impulse systems, and have continued to try them up to the present. Though appealing in terms of speed, the LVI method has never been able to match the range, resolution or repeatability and signal to noise ratio of the sweep method [7]. A detailed evaluation of the relative merits of the two methods can be found in the research works carried out in [6–16]. Given the potentials of sweep frequency analysis, this

* Corresponding author at: Department of Electrical Engineering, Engineering Faculty, Azarbaijan University of Tarbiat Moallem (AUTM), 5375171379 Tabriz, Iran. Tel.: +98 (0) 412 432 7500x2281; fax: +98 (0) 412 432 7566.

E-mail address: Behjat@azaruniv.edu (V. Behjat).

paper along with its companion (Ref. [5]) deals with development of a diagnosis approach based upon sweep frequency analysis, for detecting interturn winding faults.

In recent years, applicability and sensitivity of the SFRA method in evaluating mechanical integrity of core, windings and clamping structures within power transformers has been extensively tested by means of faults simulations in laboratory and of real cases studies of transformers in site [6–27]. However, despite its importance, research on interturn fault diagnosis using the SFRA method is rather limited. A literature review indicates that all of the contributions pertinent to the present study have concentrated only on inter-disk type faults and find it enough to show the overall changes of the frequency response of the transformer as a result of fault [28–30]. The modification of the winding frequency response as a result of inter-disk fault has neither been systematically analyzed nor reasons for it ascertained in the existing literature.

Investigating the sensitivity and feasibility of the SFRA method as a diagnostic tool to detect interturn winding faults especially low-level interturn faults in power transformers, identification of the most appropriate test configuration for this application and reliable information about the relationship between changes of the winding transfer function and interturn faults are the issues, so far, remain unreported. This research work is aimed at extending the previous studies for sensitive detection of interturn faults utilizing characteristic signatures associated with the interturn faults extracted from the SFRA records through a systematic study. The approach adopted keeps at disposal a 100 kV A, 35 kV/400 V distribution transformer on which interturn faults were imposed, and a measurement setup consisting of a network-analyzer for measuring the transfer function in the required frequency range.

While the effects of the interturn faults are known to be problematic, the current study was focused upon obtaining a better understanding of the complex physical behavior of the transformer in the presence of interturn faults. In order to see these relationships most clearly, a finite element model of the tested transformer was developed. Obviously, a correct understanding of what governs the modification of the physical behavior of the transformer as a result of interturn faults would assist in justifying the changes of winding frequency response and hence developing a reliable and sensitive fault detection method. Efforts will be made to interpret the SFRA result and quantifying the fault severity level in the shorted turns using statistical indicators.

The paper is organized as follows. Section 2 focuses on basic concepts related to SFRA method and the methodology used for doing the experiments. Section 3 presents a brief description addressing the electrical characteristics of the tested transformer and illustrates how interturn faults were staged on the windings of the transformer. The most appropriate test configuration for making sensitive SFRA measurements will be discussed in Section 4. Several characteristic signatures attained to interturn faults inferred based on the inspection of transfer function of the winding in faulty and normal operating conditions of the tested transformer and the subsequent diagnosis are illustrated in Section 5. Section 6 describes the results of applying statistical indicators to the measured SFRA records in order to provide a quantitative way for diagnosing the fault on the transformer windings. Discussion of the experimental results and implications for future researches are given in seventh section. Finally, conclusions will be presented in the last section.

2. Measurement method

The SFRA method injects sinusoidal low voltage signals of varying frequencies into one side of the winding and measures the output signals as they exit the winding in order to obtain the winding

transfer function. Treating a power transformer, undergoing SFRA, as a two-port network, the transfer function of the network is defined as the quotient of the output to input frequency responses when the initial conditions of the network are zero. Fig. 1, illustrates a basic SFRA measurement circuit including two-port network model of the transformer where Z_{ij} parameters in the model are formed by distributed resistive, capacitive, self and mutual inductive elements of the electrical equivalent circuit of the transformer. The tested impedance, in this case the impedance of the winding, is denoted by Z_{12} . In a case where the input and measured signals are generally referenced to ground; Z_{11} and Z_{22} represent the impedance paths to ground, through the bushing insulation. Z_{21} represents the impedance between the two reference grounds which in practice approaches zero because the negative terminals in the above diagram are short-circuited through the transformer tank when the transformers is tested. Finally, S is the source used for generating the input sinusoidal signal and Z_s is the impedance of the source. Conventionally, there exist two types of transfer functions which normally used in FRA analysis for diagnostic purposes: Voltage Ratio (V_{out}/V_{in}) and Impedance (V_{in}/I_{in}). It should be noted that the sensitivity of each transfer function to defects and changes in the transformer assemblies is very different. Therefore the user of the method has to find out the most sensitive transfer function for defect detection.

In this study, determination of the transfer function in the frequency domain was performed with a network-analyzer which used for generating the input sinusoidal signal, also making the voltage measurements and manipulating the results. Omicron measuring system (Bode 100) was used in the measurements carried out in this paper. The tracking generator of the network-analyzer produced an alternating voltage of 5 V in amplitude as the reference signal of the measuring system. Two leads carrying input (reference) and output (test) signals were used for the connections between the network-analyzer and the bushings at two ends of the test winding. The transformer tank and the lead ground shields were connected together to assure that no external impedance is measured and also reduce the effect of noise and the environmental effects. This measurement setup accompanied by the experimental test object which will be introduced in the following section completes the test setup for performing the SFRA measurements. In the tests reported in this paper, the measured frequency range is 100 Hz–1 MHz with 400 frequency points per decade. The use of such high number of points which lead to increasing the taken time to make each measurement is justified by the decrease in the probability of missing true resonance points and losing resolution in the approximated transfer function with the collected data points. With the used sweep settings, an SFRA scan could take a few minutes.

3. Experimental setup

SFRA measurements were carried out in high voltage laboratory on a three phase, two winding, 35 kV/400 V, 100 kV A distribution transformer with a turn ratio of 4550/60. The LV and HV windings of the transformer had layer and disk-type configurations

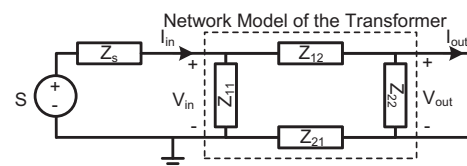


Fig. 1. Basic SFRA measurement circuit including two-port network model of the transformer.

respectively. Interturn faults were imposed on the turns of outermost layer of HV disks, which was the only accessible part of the transformer's windings. To develop interturn short circuit faults, in steps, the transformer oil was pumped out and the front wall of the transformer tank was removed to expose the windings. After the windings were allowed to dry, two conductors on the farthest layer of the second disk from the line end of the HV winding on phase "U", located at two ends of the layer, were chosen and the insulation over them at a point on each was carefully removed to make tapping points. The next step was extracting leads from the tapping points on the chosen conductors. Low impedance insulated wires were attached to the conductors by means of specific clamps embracing the conductors at the tapping points. The leads were then brought out of the transformer to allow easy access to the internal turns and also providing possibility for externally producing interturn faults. Since it was difficult to quantify exactly what number of turns involved by the fault, so after the connections were completed, the winding was energized by a low voltage power supply and the open circuit voltage between the tap conductors was recorded. This measured voltage between the taps, divided by the line to neutral value of the measured voltage applied to the winding, was an exact measure of the fraction of the winding

that was involved by the fault. The fault level that could be realized by shunting the tap conductors was equal to 0.2% of the turns on the winding which involves a very small percentage of the winding.

Before reassembling the transformer, an insulation resistance test was performed to verify that the resistance of the tap conductors to ground was greater than $1\text{ M}\Omega$. A glass wall as a replacement for front wall of the transformer tank was fixed to the tank by screw bolts and then the oil refilled. Fig. 2 shows a physical view of the tested transformer before and after refilling the oil to the transformer tank. After reassembling of the transformer, interturn faults could be staged by connecting two taps to each other through a low impedance knife switch to be able to handle the extremely high circulating fault currents flowing through the shorted turns. To adjust the fault severity in the shorted turns, a variable resistor was used in series with the switch in the conductive path between the terminals of the fault region. Various levels of fault severity could then be attained by changing the value of the fault resistance in this leakage path. The sketch in Fig. 3, illustrates an exaggerated presentation of the corresponding geometrical and circuit domain of the transformer coils and also the details of the tapping points and the staged fault on phase "U" of the transformer

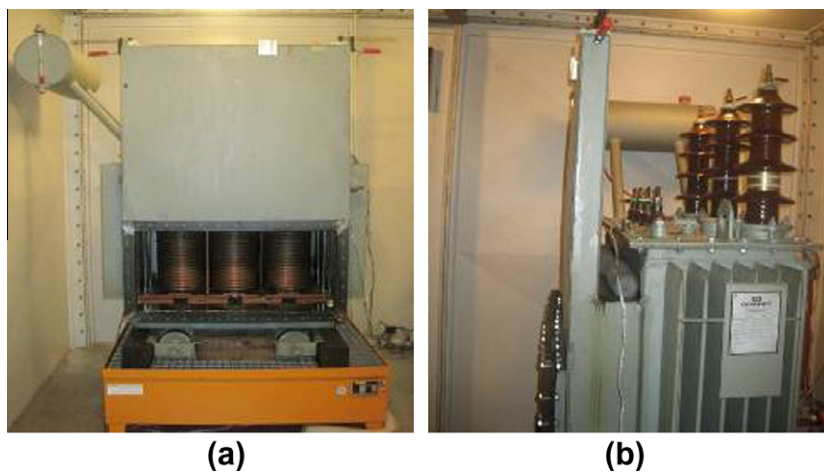


Fig. 2. (a) Front view of the tested transformer before refilling the oil and (b) Side view of the transformer after refilling the oil.

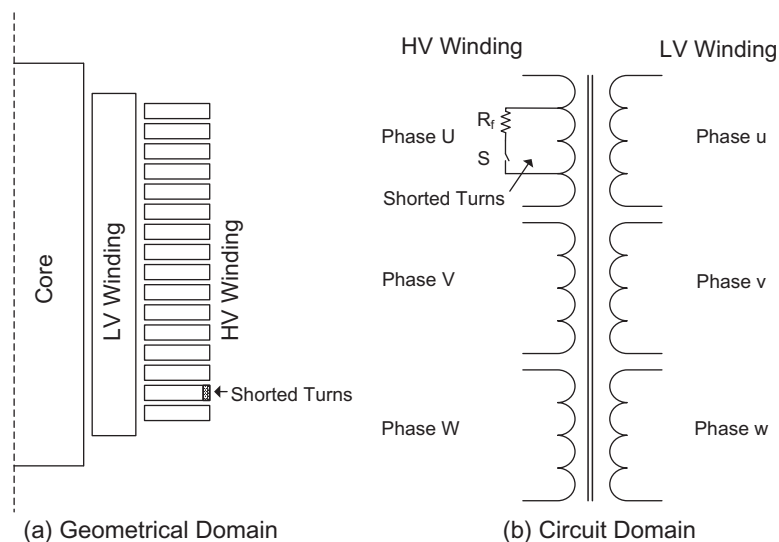


Fig. 3. Exaggerated presentation of the transformer coils and the staged fault on the 2nd disk from the line end of the HV winding on phase "U".



Fig. 4. Tap positions along the HV winding of the transformer, (a) before refilling the oil and (b) after refilling the oil to the tank.

HV winding. In the figure, the external limiting fault resistance and the time controlled switch for initiating the fault are denoted by “s” and “ R_f ” symbols respectively. A close view of the considered transformer’s HV windings and tap positions of the introduced fault, before and after refilling the oil to the transformer tank, is given in Fig. 4. Before conducting the experiments, a full-load test was performed on the transformer with the taps open to verify that the modifications had not changed the transformers’ normal operating characteristics. Once this test was completed, selected fault scenarios could be staged to make the SFRA measurements.

4. Identification of the most sensitive test configuration

An effort was made by the authors in order to identify the most appropriate configuration for making sensitive frequency response measurements. Two different transfer functions, various terminal configurations and three categories of measurement types were studied. The sensitivity of the two transfer functions, i.e. voltage gain and impedance, was investigated by analyzing the frequency responses determined by each of the methods. Once the appropriate transfer function for fault detection was identified, the next step was to determine the most appropriate combination of terminal connection and measurement type for achieving the maximum fault detection ability. Open and short circuit terminal configuration and three categories of winding measurement including high voltage, low voltage and inter-winding measurements were made to identify the most sensitive configuration for detecting winding faults. Through these studies, it was found that measuring voltage gain across HV winding of the transformer, keeping all HV and LV non-tested terminals floating, offers greater sensitivity and ability in fault detection, owing to preparing more number of resonance points and also effectively taking into account the core effects at

lower frequencies. More detailed description regarding the most suitable set of test configuration which would have the highest possible ability for interturn fault detection, can be found in the research work carried out by the authors in [31]. The following section focuses upon evaluating of the SFRA measurements in diagnosis of interturn faults on the windings of the transformers.

5. SFRA measurements

To obtain diagnosis criteria for detecting of interturn winding faults, a fault involving 0.2% turns was staged on the phase “U” of HV winding of the transformer. It should be noted that the imposed fault involves a very small percentage of the winding. As well, the smallest value of the fault resistance was chosen to account for a metal-to-metal contact and dispose of an extreme value which helped to evaluate trends. Over the course of the experimental tests, a series of experiments were conducted, in some cases with several trials of each to verify the correctness of the measurement records. Fig. 5 gives two traces collected in normal and faulty operating conditions of the transformers when the transformer is filled with oil. It is clear from the results, that the faulted response is substantially different from the non-faulted response over the low frequency range below 1 kHz.

The key point to understand the low frequency deviation caused by shorted turns can be found in explanation of Faraday’s law in the shorted turns. Faraday’s law states that the electromotive force (emf), induced in a turn equals the rate of variation of the electromagnetic flux inside it. As a well known conclusion from this law, at a fixed frequency, the amount of flux entering the turn is fixed by the emf at its terminals. From this assumption, when a short circuit occurs at a given turn, the voltage is forced to drop in it and consequently circulating current flows in the short circuited

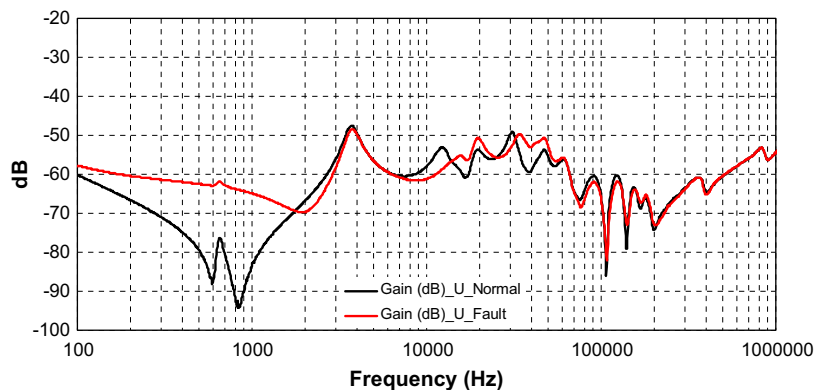


Fig. 5. Transfer function for phase “U” of the HV winding in normal and faulty operating conditions of the transformers.

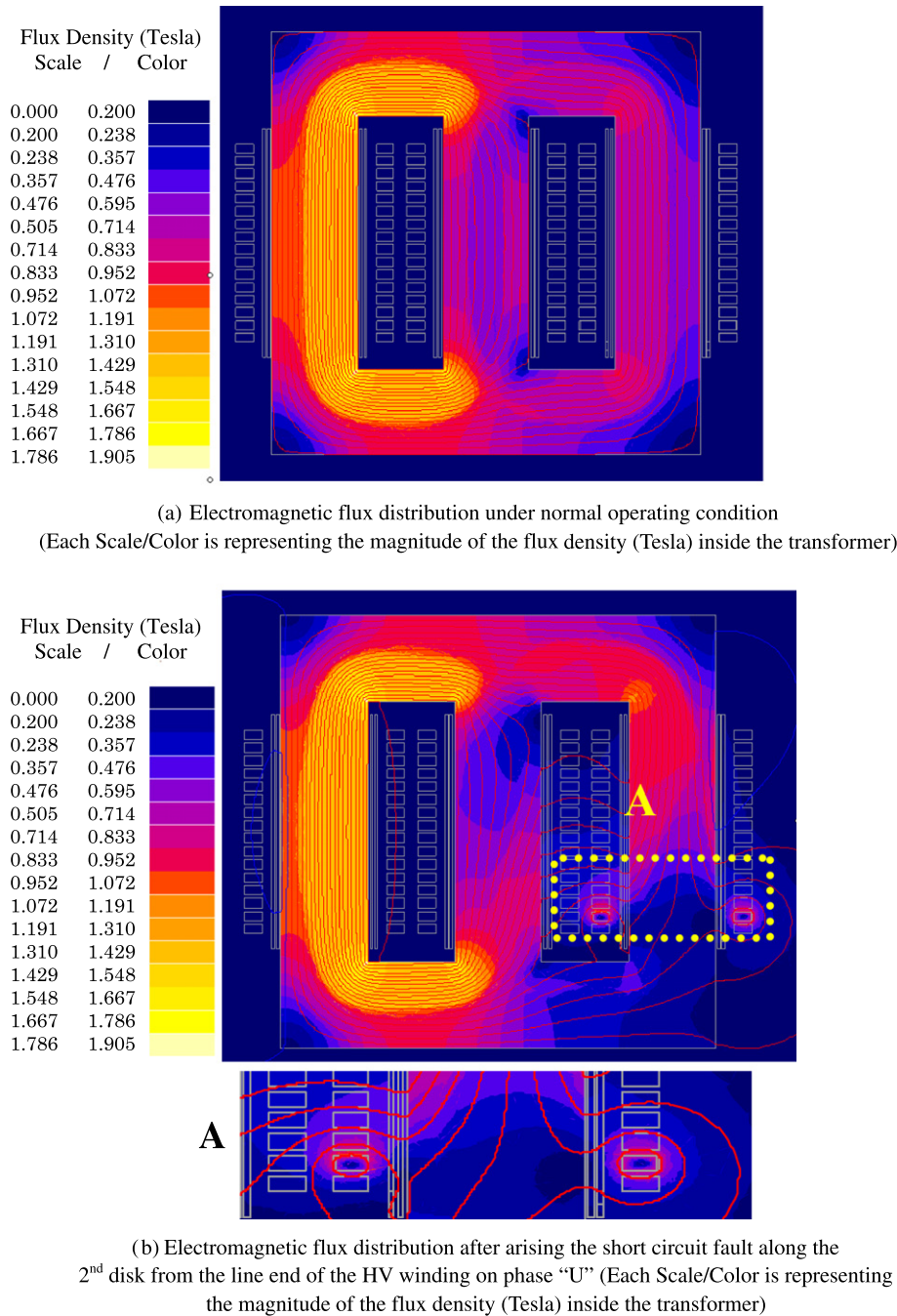


Fig. 6. Flux plot of the transformer under normal and faulty operating conditions and detail showing the damaged disk.

turn, to limit the entering flux into the turn. Let's consider an ideal situation where a turn with null resistance is short-circuited by a null fault resistance. In this condition, the shorted turn would have a null voltage at its terminals and hence no flux would enter inside its contour. The larger the fault resistance, the larger is the flux entering inside the turn. On the contrary, as the severity of the short circuit increases, means that the turns short-circuited with smaller fault resistance, a larger amount of flux would be surrounding the shorted turns.

In order to see these relationships most clearly, a finite element model of the tested transformer was developed. A description about the finite element model of the transformer and the principle used for modeling winding short circuit fault is given in appendix and more detailed description can be found in [37]. Flux plot (equiflux lines) and color shaded plot of the electromagnetic

flux density inside the studied transformer generated by FEM model of the transformer under normal operating condition and after a short circuit fault arises along one of the transformer HV winding's disks on phase “U”, with a fault resistance equal to 1 m Ω , are given in Fig. 6a and b respectively. It can be clearly seen from Fig. 6, how the distribution of the magnetic flux is fundamentally altered after the fault occurrence on the winding. There is a strong leakage flux, despite the normal leakage flux, surround the damaged turns through air paths and reduced flux lines inside the shorted turns on the core limb due to the fault occurrence. Dense flux trajectories outside the faulty region in Fig. 6b correspond to higher levels of flux density, outside the damaged turns and reduction of it on the transformer core limb as it can be clearly identified in color shaded plot of the electromagnetic flux density.

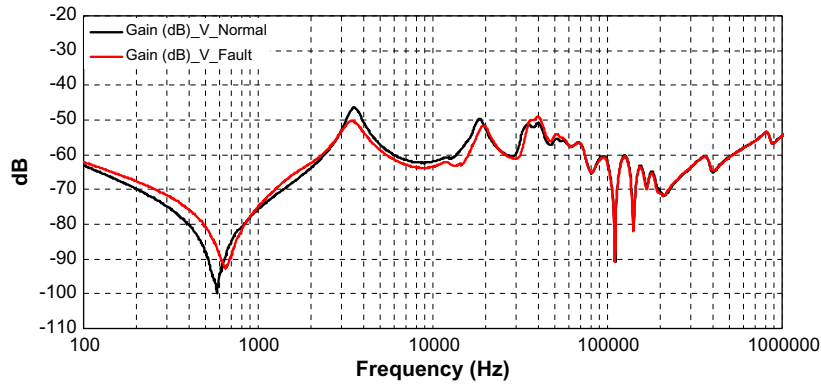


Fig. 7. Frequency response of phase “V”, before and after arising the fault on phase “U” of the HV winding.

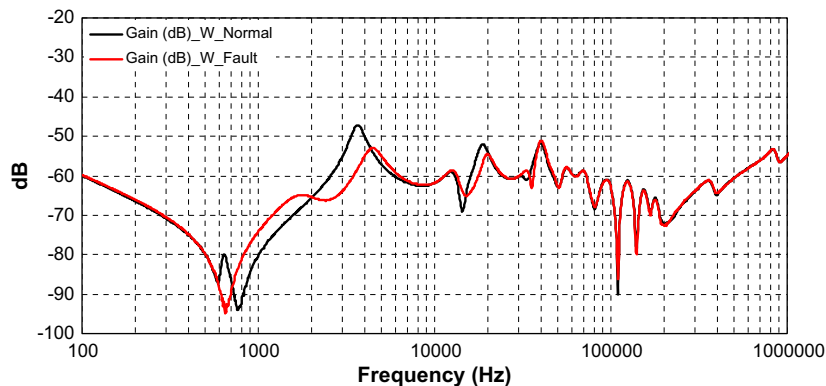


Fig. 8. Frequency response of phase “W”, before and after arising the fault on phase “U” of the HV winding.

By considering all these observations, one can conclude that the winding short circuit changes the magnetizing characteristics of the transformer core which in turn causes the low-frequency deviation of the winding frequency response. The core effect is located in the lowest frequency bandwidth on the winding frequency response, when measuring across a winding with other windings floating and not shorted [31].

Interturn faults, in addition to the changes at lower frequencies of the frequency response, also will give differences at mid-frequencies. In a range of 10 kHz up to 100 kHz the differences are very significant. As can be obviously seen from the response traces in Fig. 5, the general effect of the interturn fault is a shift of the transfer function towards higher frequencies. The movement of the resonant frequency points to the right on the response plot as a result of interturn fault occurrence is much more obvious in the frequency range of 10 kHz up to 60 kHz. Trends of increasing and decreasing absolute values of the response are also detectable in this frequency range. A closer look at the transfer function plot in Fig. 5 indicates that the magnitude of the transfer function changes as much as 6 dB in the pronounced mid-frequency resonance at around 38 kHz from the faulty case where the fault resistance is almost equal to zero to the normal response. This absolute effect is comparable to the uncertainty of the measurement. There is a linguistic agreement between some experts, that any difference within about 0.2 dB from one set of SFRA measurements to the next is usually considered as an indication of a physical change inside the transformer [38]. The normal and faulty traces are almost identical at all frequencies above approximately 100 kHz where traces overlay very well in this range.

It should be noted that although the influence of the fault on the faulted phase response is much more obvious; but the differences

of the two other phases responses as a result of fault occurrence is noticeable too. Figs. 7 and 8 present the frequency responses of phases “V” and “W” of the transformer HV winding in both normal and faulty operating conditions, retaining the same fault case considered above. Again a same type of behavior similar to the faulted phase response, i.e. movement of the transfer function to higher frequencies and changing the absolute values of the transfer function, is observed for the responses of failure-free phases. Albeit, as compared to faulted phase response which the effect of the interturn fault reaches into the midrange of the frequency response up to 100 kHz, Fig. 5, the effect of the fault is negligible above 60 kHz for Phase “V” and 25 kHz for phase “W” in their corresponding frequency responses. The effect of the fault on the low frequency range of the responses of non-faulted phases is seriously different. Figs. 7 and 8 reveal that, except removing one of the core resonance points of phase “W”, there is not any other serious modification in the low frequency responses of the non-faulted phases in spite of the drastic change in the low frequency range of the faulted phase response. Obviously this behavior is a result of the limitation of the fault effects on the core limb corresponding to the damaged winding of the transformer.

To better prove the characteristic signatures attained to interturn faults inferred based on the inspection of transfer function of the winding in faulty and normal operating conditions, additional experiments were performed with different levels of the fault severity in the shorted turns. Figs. 9–11 show the magnitude plot of the transfer functions corresponding to three phases of the transformer HV winding obtained from a frequency sweep analysis as a result of 0.2% winding short circuit on phase “U” but with different fault resistance values to create the desired fault severity level in the shorted turns.

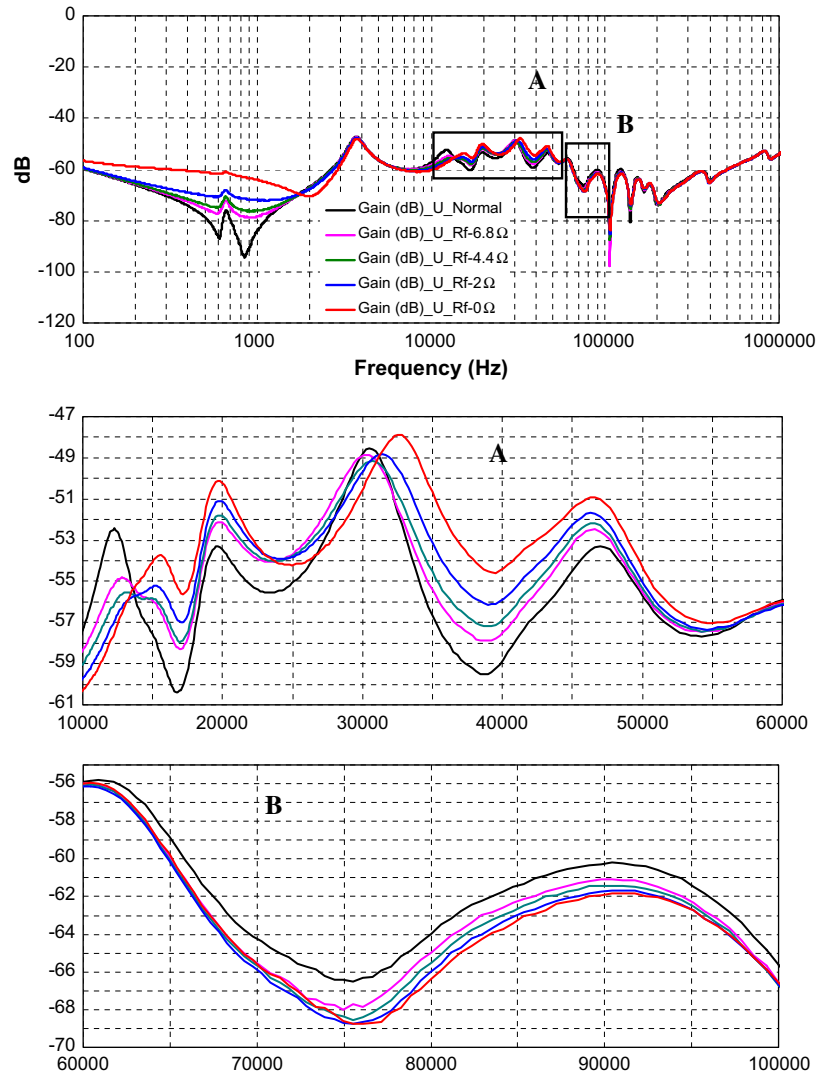


Fig. 9. Normal and faulty responses of phase “U” of the HV winding with different fault severity levels.

Considering Figs. 9–11 proves that the main characteristic features associated with interturn faults extracted from the frequency response measurements, namely displacement of the resonant frequency points to the right and a change in the transfer function magnitude are discernible for all the fault severity levels in the mid-frequency range of three phase frequency responses. Furthermore, the change in the low frequency response of the faulted phase is clearly noticeable for all the fault severity levels. A zoomed transfer function plot showing these aspects are illustrated in Figs. 9–11.

Fig. 12 illustrates the frequency response of phase “u” of the transformer LV winding before and after interturn fault occurrence on phase “U” of the HV winding. It can be clearly seen that the most important feature in regard of diagnosis is the deviation of the low frequency response of the transfer function and also creation of one new resonance point around 20 kHz as a result of fault occurrence. Modification of the low frequency response of phase “u” of the LV winding is justified by this fact that this winding is located on the same core limb which the damaged HV winding on phase “U” is located on it, so both the responses of the LV and HV windings are affected by modifications of the core in the fault region. The comparison of HV and LV winding measurements, Figs. 5 and 12, indicates that contrary to HV winding measurements,

which the effects of interturn fault reach into the midrange of the frequency response up to 100 kHz, in LV winding measurements, high frequencies above 40 kHz are not affected by the fault.

Fig. 13 shows the SFRA results, taken by inter-winding measurements having the terminal of phase “U” of the HV winding as input and the corresponding terminal on the phase “u” of the LV winding as output, prior and after interturn fault occurrence on the phase “U” of the HV winding. While reviewing the trace from left to right, a partial difference is seen between normal and faulty responses starting from just above 10 kHz and continuing to around 45 kHz in the form of shifting the resonance points to the right and changing the absolute values of the transfer function. However there is not a visible fault indication in the low frequency range of the transfer function which looks very different to the HV and LV winding measurements described in previous sections. In fact, such a behavior is not surprising, as the low frequency deviation in the winding response as a result of interturn fault is governed by the interaction between core and windings while the inter-winding measurement is made with almost no reference to the core effects at lower frequencies as discussed earlier.

To give a better idea about sensitivity of the proposed diagnostic method and the real condition of the transformer under different interturn faults considered in Figs. 9–11, it should be noted

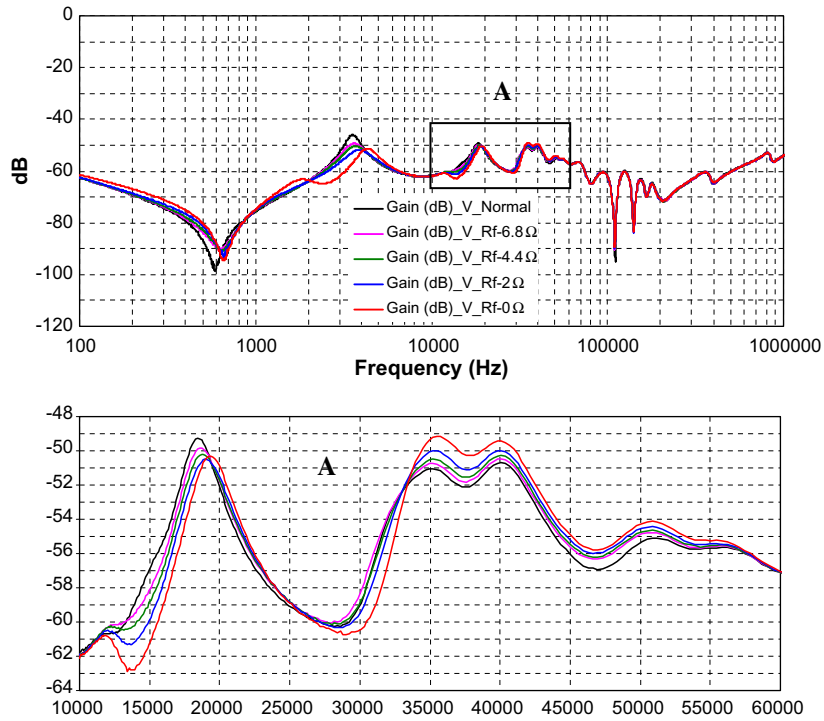


Fig. 10. Response of phase “V”, before and after arising the fault with different severity levels on phase “U” of the HV winding.

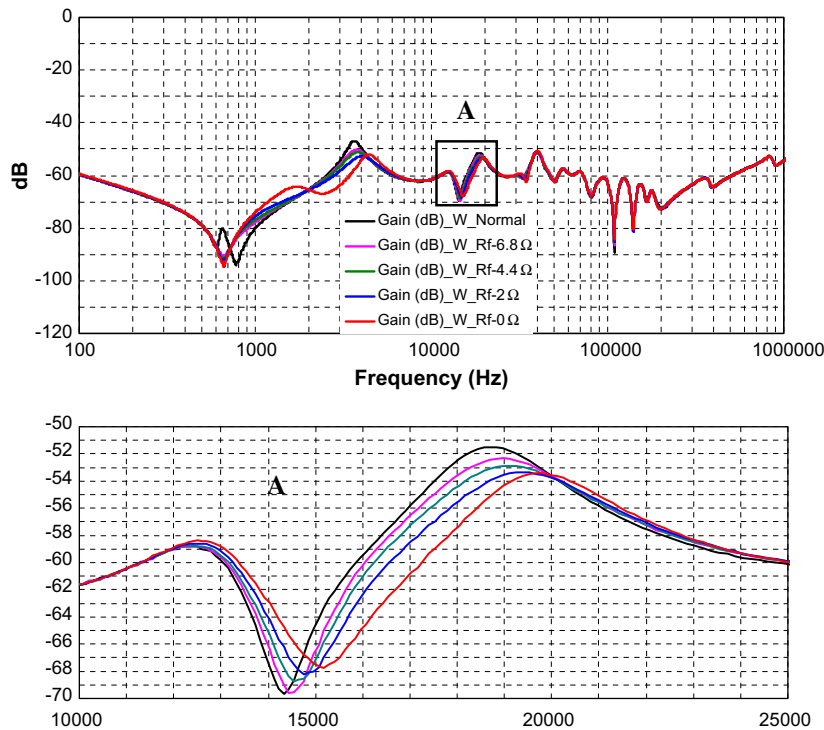


Fig. 11. Response of phase “W”, before and after arising the fault with different severity levels on phase “U” of the HV winding.

that the faults with resistance values of 0Ω , 2Ω , 4.4Ω and 6.8Ω cause a differential current of only 11.5%, 1.56%, 0.85% and 0.59% rated current respectively under full load conditions of the transformer which makes detection of these fault by traditional transformer protection devices to a very challenging task. The measurements performed in this section proves the observations made in Ref. [31] that the voltage gain transfer function when

measuring across a HV winding with other windings floating and not shorted is more sensitive to interturn winding faults. In addition, the deviation of the low frequency response of the LV winding located on the same phase of the damaged HV winding is large enough to indicate the fault occurrence. It is also proved that the inter-winding measurement is less effective in detecting interturn faults as compared to the two other HV and LV categories.

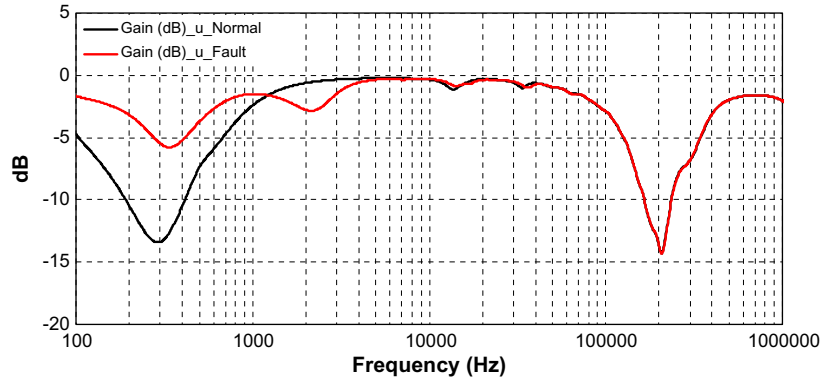


Fig. 12. Response of phase “u” of the LV winding before and after arising the fault on phase “U” of the HV winding.

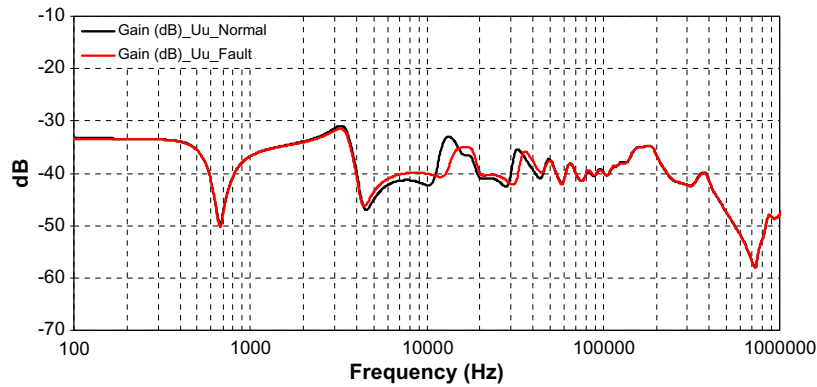


Fig. 13. Response of phase “U” by inter-winding measurement before and after arising the fault on phase “U” of the HV winding.

6. Interpretation of the results

The SFRA provides a wealth of information in the form of a frequency response plot, which needs to be interpreted. It was shown that interturn faults produce changes in the winding transfer function at different frequency intervals, thereby providing some discriminating features. Overall changes in the response traces, shifted resonances, new created or removed resonance points and amplitude differences are the main features extracted from the frequency response measurements. Although, comparing the differences of the faulted and non-faulted responses of the winding based on the extracted features, provides some clear indication regarding the fault occurrence, but the main problem with this method of comparison is that the diagnosis task is performed by expert's judgment through the visual inspection of the records and hence strongly depends to the expert's opinion. Furthermore, the method cannot be easily incorporated in an automated detection procedure. The use of statistical indicators can solve this problem, giving support to interpretation of the results and making it more objective and transparent. Some statistical parameters such as: correlation coefficient, spectrum deviation and maximum absolute difference have been proposed by some researches in the past in order to establish the differences between recordings of the SFRA measurements [39–43]. Correlation coefficient and spectrum deviation as two statistical indicators, are used in this study for comparing the SFRA traces. The corresponding mathematical expression of these parameters are given by:

$$\rho = \frac{\sum_{i=1}^n x_i y_i}{\sqrt{\sum_{i=1}^n x_i^2 \sum_{i=1}^n y_i^2}} \quad (1)$$

$$\sigma = \frac{1}{n} \sum_{i=1}^n \sqrt{\left(\left[\frac{x_i - (x_i + y_i)/2}{(x_i + y_i)/2} \right]^2 + \left[\frac{y_i - (x_i + y_i)/2}{(x_i + y_i)/2} \right]^2 \right)} \quad (2)$$

where $X(x_1, x_2, \dots, x_n)$ and $Y(y_1, y_2, \dots, y_n)$ are two sets of n numbers, ρ is the correlation coefficient and σ is the spectrum deviation between these two sets. In investigating the relationship between two signals, the highest possible similarity level is obtained by correlation coefficient equal to unity and spectrum deviation to zero. Table 1 shows the correlation and spectrum deviation between the faulted and non-faulted responses of phase “U” of the HV winding, calculated in decade frequency bands. The calculated indicators given in Table 1, are corresponding to the measurements which were shown previously in Fig. 5. In complete agreement with the measured traces in Fig. 5., it can be clearly seen from the table that the largest deviation or smallest correlation values are related to the lowest frequency band of the responses, i.e. 100 Hz–1 kHz, where is much affected by the interturn fault. Also, the upper zero values of the spectrum deviation and under unity values of the correlation coefficient in the 1–10 kHz and 10–100 kHz frequency bands indicate to differences between the faulted and non-faulted responses at medium frequencies. As obvious from the table, the indicators illustrate good agreement between the responses from 100 kHz up to 1 MHz which proves that the high frequencies are not affected by the interturn fault.

Comparing the corresponding values of the two considered indicators in Table 1, also proves the higher sensitivity and reliability of the spectrum deviation as a statistical indicator in detecting interturn faults. In fact, it was found through the author's trials that the differences between the normal and faulty responses of the transformers windings damaged by interturn faults, is more re-

flected in the spectrum deviation as compared to the correlation coefficient. As seen in Table 1, all the correlation values are acceptably around unity in all the frequency bands, however the value of the spectrum deviation in the 100 Hz–1 kHz band is large enough to indicate the interturn fault occurrence.

Table 2 shows the correlation and spectrum deviation between the faulted and non-faulted responses of three phases of the transformer HV winding, corresponding to the traces previously shown in Figs. 5, 7 and 8. It is seen from the table that the largest differences between the faulted and non-faulted traces are clearly related to the damaged phase “U”. The corresponding values of the undamaged phases of the transformer HV winding, i.e. “V” and “W” phases show a similar trend to the damaged phase throughout all the frequency bands. However, the lower values of the spectrum deviation coefficients for the undamaged phases as compared to the corresponding value of the damaged phase in the same frequency bands, amounts to a reduced effect of the fault on the non-damaged phases.

Table 3 illustrates the results of applying the indicators to the normal and faulty responses of phase “u” of the transformer taken by HV, LV and inter-winding measurements. The corresponding

measurement results were shown previously in Figs. 5, 12 and 13. The spectrum deviation for the responses related to the LV winding reaches high values in the 100 Hz–1 kHz and 1–10 kHz decade bands, where the changes caused by the interturn fault are most apparent. The spectrum deviation between results from inter-winding measurement are very close to zero throughout all the frequency bands. This is a good indication of less sensitivity of inter-winding measurement in detecting interturn faults which described in detail in previous sections.

As seen, the use of the statistical coefficients of the SFRA records can provide a quantitative way for diagnosing the presence of the fault, complementing the previous qualitative approaches. In addition to the benefits gained from adding more objectivity and transparency to interpretation of the SFRA results, significant advantages would accrue by quantifying the fault severity level through the use of coefficients. Table 4 shows the correlation and spectrum deviations between the baseline measurement of the phase “U” of HV winding and four measurements made during the fault occurrence with different severity levels on the same winding. The results in Table 4 illustrate how the spectrum deviation of the faulty responses with the baseline measurement increases with increasing of the fault severity in the shorted turns. This fact allows the quantification of the fault severity level. It has to be highlighted that the reliability of the fault diagnosis is achieved by means of the qualitative approach based on the detection of the characteristic patterns that appear in the frequency response of the windings during the fault occurrence. Once the fault is identified, the computation of the statistical coefficients allows the quantification of the degree of fault. So both approaches together make possible the detection of the presence of the fault and its quantification and hence ensure giving the proper diagnosis.

Table 1
Correlation (ρ) and spectrum deviation (σ) between the faulted and non-faulted responses of phase “U” of the HV winding.

Frequency decade	ρ	σ
100 Hz–1 kHz	0.9951	0.1204
1–10 kHz	0.9968	0.0434
10–100 kHz	0.9983	0.0342
100 kHz–1 MHz	0.9998	0.0068

Table 2
Correlation (ρ) and spectrum deviation (σ) between the faulted and non-faulted responses of three phases of the HV winding for a fault on phase U.

Frequency decade	Phase “U”		Phase “V”		Phase “W”	
	ρ	σ	ρ	σ	ρ	σ
100 Hz–1 kHz	0.9951	0.1204	0.9991	0.0281	0.9985	0.0170
1–10 kHz	0.9968	0.0434	0.9995	0.0193	0.9968	0.0326
10–100 kHz	0.9983	0.0342	0.9994	0.0178	0.9994	0.0130
100 kHz–1 MHz	0.9998	0.0068	0.9999	0.0031	0.9999	0.0024

Table 3
Correlation (ρ) and spectrum deviation (σ) between normal and faulty responses of phase “U” taken by HV, LV and inter-winding measurements.

Frequency decade	HV		LV		Inter-Winding	
	ρ	Σ	ρ	σ	ρ	σ
100 Hz–1 kHz	0.9951	0.1204	0.9817	0.6040	0.9999	0.0010
1–10 kHz	0.9968	0.0434	0.7721	0.4625	0.9997	0.0119
10–100 kHz	0.9983	0.0342	0.9943	0.0866	0.9985	0.0254
100 kHz–1 MHz	0.9998	0.0068	0.9999	0.0029	0.9999	0.0011

Table 4
Correlation (ρ) and spectrum deviation (σ) between normal and faulty responses of phase “U” of the HV winding in presence of faults with different severity levels.

Frequency decade	Fault impedance (R_f)							
	6.8 Ω		4.4 Ω		2 Ω		0 Ω	
	ρ	σ	ρ	σ	ρ	σ	ρ	σ
100 Hz–1 kHz	0.9987	0.0257	0.9981	0.0349	0.9968	0.0560	0.9951	0.1204
1–10 kHz	0.9998	0.0050	0.9997	0.0078	0.9991	0.0149	0.9968	0.0434
10–100 kHz	0.9997	0.0142	0.9995	0.0181	0.9992	0.0244	0.9983	0.0342
100 kHz–1 MHz	0.9998	0.0049	0.9999	0.0056	0.9998	0.0065	0.9998	0.0068

7. Discussion

The experiments presented in previous sections suggest the capability of the SFRA method as a diagnostic tool to detect interturn winding faults. According to the applied tests the sensitivity of the SFRA method can recognize an interturn fault involving 0.2% of turns on the transformer winding. As an outcome of these studies, the following points can be summarized. Measuring voltage gain across the HV winding of the transformer constitute the appropriate pair of system function and measurement type, because of preparing the maximum number of natural frequencies and so significantly improving the achievable sensitivity. Interturn faults along the winding will cause significant changes in the magnetic behavior of the transformer and hence give deviation in the low frequency range of the frequency response where is much affected by the magnetic core. Since by shorting out the non-tested terminals the measurement is made with almost no reference to the magnetic core, so it is strongly recommended to use floating terminal configuration for achieving highest possible ability for detecting of interturn fault.

The SFRA is a relative method means that an evaluation of the transformer condition is done by comparing an actual set of SFRA results to reference results; three types of comparison for measurement results can be realized. The highest level of comparability is obtained by using a former fingerprint measurement made on the same winding earlier in a time-based comparison. However, it is unlikely that we ever get a baseline for all transformers on the electric supply network. Consequently, other comparison strategies which involve sister units or inter-phase comparison are used. Although, slight differences may be found between sister transformers, owing to the effect of manufacturing differences in the windings and asymmetries brought in through construction, but it is particularly useful when there is no fingerprint measurement available. The least reliable method is inter-phase comparison, due to significant differences between windings on different phases of three-phase transformers especially at low frequencies, itself a function of differences in the magnetizing inductance between the three phases. The center phase, as illustrated in Figs. 5, 7 and 8, exhibits deviation from the two outer phases at lower frequencies. Then it may be advisable to make inter-phase comparison for just the two outer phases.

In the experiment carried out in this paper on a distribution transformer, some useful characteristic signatures associated with interturn faults were extracted from the measurement records in order to obtain diagnosis criteria for detecting winding interturn faults. However, more detailed studies and exhaustive tests on numerous power transformers is needed to better prove the ability of the method in reliable and sensitive detection of interturn faults on power transformers well before such faults lead to a catastrophic failure with serious damage to the transformer. This issue can be done as an extension to the present work.

The performed experiments in this study proved that the structure and shape of transfer function appears to be a function of the type, overall physical size and complexity of the transformer winding. Two types of windings namely, disk type HV winding and layer-type LV winding, were investigated in this study. Future work ought to focus on interleaved winding, to extract certain features specific to the transfer function corresponding to this type of winding. Also, more exhaustive tests on numerous power transformers, in particular transformers with different configurations of LV and HV windings such as layer-type LV winding and disk-type LV winding is highly desirable in the future works to establish more reliable and sensitive diagnosis approach for interturn fault detection on the transformer windings.

In spite of many research efforts on fault diagnosis using SFRA method, there is still no universally accepted and systematic interpretation technique for these tests and 'expert opinion' is often sought when any damaging trend is observed as a result of fault occurrence. The authors were involved in this study in promoting the interpretation process of the SFRA results by extracting characteristic signature attained to interturn faults and thereafter using statistical indicators. The correlation coefficient and spectrum deviation were used in this study to calculate the amount of agreement or disagreement between the two sets of faulty and normal measurements for quantitative explanation of the fault presence on the transformer windings. Spectrum deviation was found to be more effective than correlation coefficient in establishing the differences between the recordings of the SFRA measurements. Exploring some other types of statistical indicators suitable for this application would be one of the future directions of this research.

8. Conclusion

Successful operation of SFRA method in precisely detecting interturn winding faults with a sensitivity of better than 0.2% of

turns along the winding, was described on a real distribution transformer. Even though SFRA measurement has been increasingly used in recent years to assess mechanical integrity of transformers, yet this contribution is novel and of practical relevance since detection of interturn winding faults and especially low-level faults on actual windings has not been reported so far. A method which assures sufficient reproducibility of the SFRA measurements was explained. The experiments on a distribution transformer for estimating the sensitivity of different transfer functions in detecting of interturn faults were the first results. It was found through the experiments that the voltage gain measurement across the HV winding of the transformer with other windings floating and not shorted is the most appropriate configuration for detecting interturn faults along the windings.

An effort was made to obtain a correct understanding of what governs the modifications of the winding transfer function as a result of fault occurrence by developing a FEM model of the tested transformer. Shifting the resonance points to higher frequencies and amplitude differences are general effects of the interturn faults on the winding frequency response. Also, the low frequency measurements proved to be very helpful for accurately monitoring the health condition of the transformer windings. To give support to interpretation of the SFRA results, and also quantifying the discriminative features associated with the interturn faults, statistical indicators were used. The spectrum deviation and correlation coefficient proved to be effective tools to provide quantitative ways for diagnosing and, at the same time, to quantify the degree of the fault severity in the shorted turns. Although, it was found that the differences between the normal and faulty responses of the transformers windings damaged by interturn faults, is more reflected in the spectrum deviation as compared to the correlation coefficient. It is believed, based on the present findings, that the SFRA method can provide an effective interpretation of transformer performance, in terms of early fault detection. However, this method must be considered as an additional tool in conjunction with other diagnostic tests to more precisely detect the fault on the windings.

Acknowledgment

The authors are highly grateful to the Schering Institute of Leibniz Universität Hannover for the provision of test facilities and great support for experimental tests.

Appendix A

The principle used in this study to model short circuit faults on the transformer windings is to divide the winding across which the fault occurs in two parts: the short-circuited part and the remaining coils in the circuit [37]. The magnetic field inside the transformer is governed by the well-known Maxwell equations. Although, when a fault occurs inside the transformer, the magnetic flux distribution is fundamentally altered as well as the current in the circuit domain. But, the transformer terminal behavior still satisfies the governing equations. Thus, obtaining the faulty transformer behavior is achieved by solving these equations. FEM is applied here in order to solve electromagnetic field problems described by the Maxwell equations in both normal and faulty conditions of the transformer. In the two-dimensional problem considered here for the analysis of the transformer under normal and faulty conditions, the electromagnetic field and circuit coupled approach based on the A-V-A formulation was given [44]. The tested transformer was employed in simulations with all parameters and configuration provided by the manufacturer and real measurements in the laboratory. To obtain a unique solution for the

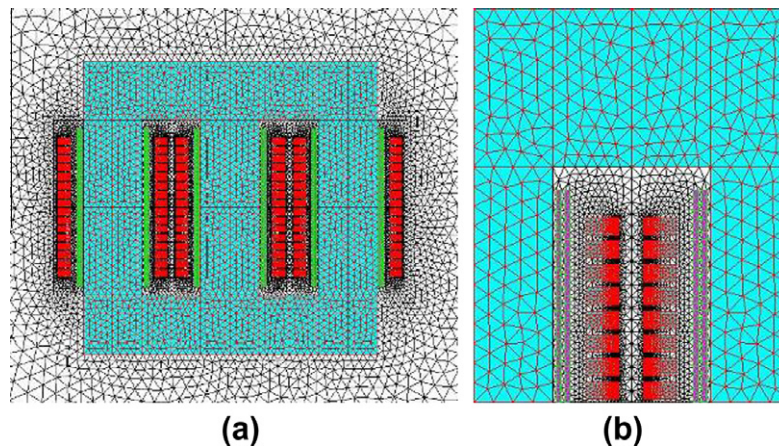


Fig. 14. (a) Finite element model of the studied transformer and (b) detail showing the fully meshed coil conductors.

governing equation based on A-V-A formulation, the zero Dirichlet boundary condition was adopted on the external circle of infinite region surrounding the transformer. Neglecting the stray losses in the transformer tank walls, the transformer tank was excluded in the computation domain. The core and surrounding oil were entirely included in the model. The nonlinear characteristics of the core was input manually into the solver and assigned to the core. HV windings of the considered transformer which have a value of skin depth much greater than the dimensions of the conductor's cross section were modeled by stranded coil conductors. However, LV windings with conductors having dimensions of cross section comparable to the value of the skin depth were modeled by solid conductors. All the coil regions in the finite element model were coupled to the circuit domain. The finite element model of the studied power transformer is composed of 52,514 surface and 10,846 line elements and includes 105,091 nodes. The meshes were constructed by using adaptive refinement techniques; so that meshes are much more refined in zones of strong variation and high intensity of the magnetic field than in the zone close to the computation domain boundary. A mesh generator that creates second order triangular elements was used for meshing of the core, surrounding oil, windings and the boundary domain. Fig. 14 represents the finite element model of the studied transformer. More detailed description regarding the FEM model of the transformers damaged by interturn winding faults can be found in [37].

References

- [1] Aggarwal RK, Mao P. Digital simulation of the transient phenomena in high voltage power transformers with particular reference to accurate fault detection. In: Internal conference on SIMULATION, conference publication no.457, IEE September–October 1998; 1998. p. 390–7.
- [2] Vahedi Abolfazl, Behjat Vahid. Online monitoring of power transformers for detection of internal winding short circuit faults using negative sequence analysis. *Eur Trans Electr Power* 2011;21(1):196–211.
- [3] Behjat Vahid, Vahedi Abolfazl. A DWT-based approach for detection of interturn faults in power transformers. *COMPEL: The Int J Comput Math Electr Elect Eng* 2011;30(2):483–504.
- [4] Georgilakis PS. Condition monitoring and assessment of power transformers using computational intelligence. In: Tang WH, Wu QH, editors. *Int J Elect Power Energy Syst*, vol. 33(10). London: Springer; 2011. p. 1784–5.
- [5] Behjat Vahid, Vahedi Abolfazl, Setayeshmehr Alireza, Borsi Hossein, Gockenbach Ernst. Diagnosing shorted turns on the windings of power transformers based upon online FRA using capacitive and inductive couplings. *IEEE Trans Power Deliv* Oct. 2011;26(4):2123–33.
- [6] Dick EP, Erven CC. Transformer diagnostic testing by frequency response analysis. *IEEE Trans Power Apparatus Syst* 1978;PAS-97(6):2144–53.
- [7] Sweetser C, McGrail T. Sweep frequency response analysis transformer applications. A technical paper from double engineering; 2003.
- [8] Wang M, Vandermaar AJ, Srivastava KD. Review of condition assessment of power transformers in service. *IEEE Electr Insulation Mag* 2002;18(6):12–25.
- [9] Lapworth JA, Jarman PN, Funnell IR. Condition assessment techniques for large power transformers. In: Second international conf. reliability of transmission and distribution equipment, Coventry, U.K., conference publication no. 406; 1995. p. 85–90.
- [10] Vaessen PTM, Hanique E. A new frequency response analysis method for power transformers. *IEEE Trans Power Deliv* 1992;7(1):384–91.
- [11] Xiaowei L, Qiang S. Test research on power transformer winding deformation by FRA method electrical insulating materials. In: IEEE proceedings of 2001 international symposium (ISEIM 2001); 2001. p. 837–40.
- [12] Tenbohlen S, Uhde D, Poittevin J, Sundermann U, Borsi H, Werle P, et al. Enhanced diagnosis of power transformers using on- and off-line methods: results, examples and future trends. Session 2000 © CIGRÉ Paris 12-204; 2000.
- [13] Ryder SA. Diagnosing transformer faults using frequency response analysis. *IEEE Electr Insul Mag* 2003;19(2):16–22.
- [14] Coffeen L, Hildreth J. A new development in power transformer frequency response analysis to determine winding deformation without the need for comparison to historical data [the objective winding asymmetry test]. In: proceedings of EPRI substation equipment diagnostics conf. X, San Antonio, TX; 2002.
- [15] Tenbohlen S, Ryder SA. Making frequency response analysis measurements: a comparison of the swept frequency and low voltage impulse methods. In: XIIIth international symposium on high voltage engineering, Netherlands; 2003.
- [16] Secue JR, Mombello E. Sweep frequency response analysis (SFRA) for the assessment of winding displacements and deformation in power transformers. *Electr Power Syst Res* 2008;78(6):1119–28.
- [17] Leibfried T, Feser K. Monitoring of power transformers using the transfer function method. *IEEE Trans Power Del* 1999;14(4):1333–41.
- [18] Feser K, Christian J, Neumann C, Sundermann U, Leibfried T, Kachler A, et al. The transfer function method for detection of winding displacements on power transformers after transport, short circuit or 30 Years of service. *CIGRE paper* 12/33-04; 2000.
- [19] Lech W, Tyminski L. Detecting transformer winding damage—the low voltage impulse method. *Electr Rev* 1966;179(21):768–72.
- [20] Malewski R, Poulin B. Impulse testing of power transformers using the transfer function method. *IEEE Trans Power Deliv* 1988;3(2):476–89.
- [21] Wang M, John Vandermaar A, Srivastava KD. Improved detection of power transformer winding movement by extending the fra high frequency range. *IEEE Trans Power Deliv* 2005;20(3):1930–8.
- [22] Rahimpour Ebrahim, Christian Jochen, Feser Kurt, Mohseni Hossein. Transfer function method to diagnose axial displacement and radial deformation of transformer windings. *IEEE Trans Power Deliv* 2003;18(2):493–505.
- [23] Satish L, Jain Anurag. Structure of transfer function of transformers with special reference to interleaved windings. *IEEE Trans Power Deliv* 2002;17(3):754–60.
- [24] Florowski Marek, Furgal Jakub. Modelling of winding failures identification using the frequency response analysis (FRA) method. *Electr Power Syst Res* 2009;79(7):1069–75.
- [25] Pleite Jorge, González Carlos, Vázquez Juan, Lázaro Antonio. Power transformer core fault diagnosis using frequency response analysis. In: Spain: IEEE MELECON, Benalmádena (Málaga); 2006. p. 1126–9.
- [26] Christian J, Feser K, Sundermann U, Leibfried T. Diagnostics of power transformers by using the transfer function method. In: Proceedings of IEEE international symposium on high voltage engineering, conference publication no. 467; 1999. p. 37–40.
- [27] Kim Jong-Wook, Park ByungKoo, Jeong Seung Cheol, Kim Sang Woo, Park PooGyeon. Fault diagnosis of a power transformer using an improved frequency-response analysis. *IEEE Trans Power Deliv* 2005;20(1):169–78.

- [28] Islam Syed Mofiml. Detection of shorted turns and winding movements in large power transformers using frequency response analysis. In: IEEE PES, winter meeting, vol. 3, Singapore; 2000. p. 2233–8.
- [29] Islam S, Ledwich G. Locating transformer faults through sensitivity analysis of high frequency modeling using transfer function approach. In: Proceedings of IEEE international symposium on electrical insulation, Montreal, Quebec, Canada; 1996. p. 38–41.
- [30] Satish L, Sahoo Subrat K. Locating faults in a transformer winding: an experimental study. *Electr Power Syst Res* 2009;79(1):89–97.
- [31] Behjat V, Vahedi A, Setayeshmehr A, Borsi H, Gockenbach E. Identification of the most sensitive frequency response measurement technique for diagnosis of interturn faults in power transformers. *Meas Sci Technol* 2010;21:1–14.
- [37] Behjat V, Vahedi A. Numerical modelling of transformers interturn faults and characterising the faulty transformer behavior under various faults and operating conditions. *IET Electr Power Appl* 2011;5(5):415–31.
- [38] McGrail Tony, Sweetser Charles. Experience with SFRA for transformer diagnostics. A technical paper from *doble engineering*; 2003.
- [39] Xu DK, Fu CZ, Li YM. Application of artificial neural network to the detection of the transformer winding deformation. In: Proceedings of high voltage engineering symposium, London, UK; 1999. p. 5.220.P5–5.223.P5.
- [40] Bak-Jensen J, Bak-Jensen B, Mikkelsen SD. Detection of ageing phenomena in transformers by transfer functions. *IEEE Trans Power Deliv* 1995;10(1):308–14.
- [41] Ryder SA. Methods for comparing frequency response analysis measurements. In: Proceedings of IEEE international symposium on electrical insulation, Boston, Massachusetts; 2002. p. 187–90.
- [42] Nafar Mehdi, Niknam Taher, Gheisari Amirhossein. Using correlation coefficients for locating partial discharge in power transformer. *Int J Electr Power Energy Syst* 2011;33(3):493–9.
- [43] Vahidi B, Ghaffarzadeh N, Hosseinian SH. A wavelet-based method to discriminate internal faults from inrush currents using correlation coefficient. *Int J Electr Power Energy Syst* 2010;32(7):788–93.
- [44] Kumbhar Ganesh B, Mahajan Satish M. Analysis of short circuit and inrush transients in a current transformer using a field-circuit coupled FE formulation. *Int J Electr Power Energy Syst* 2011;33(8):1361–7.